Journal of Cleaner Production 204 (2018) 355–365

Contents lists available at ScienceDirect

Journal of Cleaner Production

journal homepage: www.elsevier.com/locate/jclepro

Development of a low-cost PV system using an improved INC algorithm and a PV panel Proteus model

Saad Motahhir*, Abdelilah Chalh, Abdelaziz El Ghzizal, Aziz Derouich

EST, SMBA University, Fez, Morocco

ARTICLE INFO

Article history:
Received 31 May 2018
Received in revised form
16 August 2018
Accepted 23 August 2018
Available online 7 September 2018

Keywords:
Arduino uno
Low-cost
Mathematical division calculations
Modified incremental conductance
PV panel
Proteus

ABSTRACT

This paper proposes a photovoltaic (PV) model for the design of PV systems with a simple MPPT to achieve high efficiency, faster response and low cost. First, a PV panel model is developed using SPICE code in Proteus tool. The verification and the validation are performed via an experimental test bench. Afterwards, a new modified Incremental Conductance (INC) algorithm is introduced. The proposed algorithm avoids the high number of the mathematical divisions used in the conventional INC. Both methods are implemented in the low-cost Arduino Uno board using the simulated PV panel model. The results show that the modified method presents good performances regarding response time (0.1 s), steady-state oscillation, and efficiency (98.5%). To validate the proposed system, a hardware testbench is implemented using the low-cost ATMega328 microcontroller in the Arduino Uno board. Substantial cost reduction has been attained proving the financial competitiveness of the proposed controller.

1. Introduction

It is widely admitted that the use of fossil energy resources such as the petroleum and gas is condemned to fade. To meet the future energy demands, sustainable and renewable energy sources provide the next generation solutions. Among others, solar energy is of paramount interest since it is the most abundant and reliable source (Bayrak et al., 2017). Clean energy can be generated simply using photovoltaic (PV) devices (Koofigar, 2016). However, PV systems still present low efficiencies and high costs (Li et al., 2017). Therefore, intensive research efforts have been made to improve the performance of PV converters, increase their efficiency and decrease their production cost (Marinić-Kragić et al., 2018; Nižetić et al., 2018). Furthermore, the nonlinear behavior of the PV panel and its high dependency to outdoor climatic conditions and load characteristic lead to the most challenging task for optimizing the PV energy (Gupta et al., 2016). One of the solutions proposed in the literature to overcome this challenge is to operate the PV panel at the maximum power point (MPP). Which is why, various maximum power point tracking (MPPT) algorithms have been suggested (Ahmed and Salam, 2016; Faramarz et al., 2017; Gupta et al., 2016; Rezk and Eltamaly, 2015). The obvious way to assess the performance of MPPT algorithm is to test it under controllable climatic conditions. Such conditions are not easily obtained due to randomly environmental meteorological data. For that, PV emulators are generally used instead of PV panels (Kadri et al., 2012; Zakzouk et al., 2013; Zhou et al., 2014). Nevertheless, PV emulators are not always available and they are expensive, especially for developing countries (Ram et al., 2018). Alternatively, researchers use PSIM or Matlab/Simulink environments to implement and verify the performance of MPPT algorithms (Chen et al., 2016; Motahhir et al., 2017a; Rahrah et al., 2015; Rezk and Eltamaly, 2015). However, these tools do not contain embedded boards or microcontrollers (like PIC, DSP, Arduino or FPGA …) in which the MPPT algorithm can be implemented and tested as made using a real physical prototype. In turn, Proteus is the unique tool which offers the ability to simulate electrical systems through hardware components as microcontrollers, DSP, FPGA, embedded boards like Arduino, sensors, and actuators. With Proteus, the system can be simulated using hardware components and debug it by detecting the maximum of errors without the necessity of having a physical prototype. As it is well known, Proteus does not provide a PV panel model. For the first time in the literature, the one diode PV model is implemented in Proteus. To justify the model validity, an experimental setup has been constructed. The resulting benefit is that the MPPT algorithm can be implemented using the hardware components provided by Proteus. Consequently, this solution can be used as a low-cost PV simulator when the physical prototype is not

* Corresponding author.
E-mail address: saad.motahhir@usmba.ac.ma (S. Motahhir).

https://doi.org/10.1016/j.jclepro.2018.08.246
0959-6526/

Nomenclatures

a	diode's ideality factor
F	switching frequency [Hz]
I	panel output current [A]
I_s	diode saturation current [A]
I_{ph}	photocurrent of the panel [A]
G	solar irradiation [W/m^2]
k	Boltzmann constant [J.K^{-1}]
q	electron charge [C]
R_{ds}(on)	Static Drain-to-Source On-Resistance of the switch transistor [Ω]
R_s	series resistance [Ω]
R_{sh}	shunt resistance [Ω]
T	junction temperature [K]
V	photovoltaic voltage [V]
V_d	output of voltage divider circuit [V]
V_o	output voltage of the Boost converter [V]
I_o	output current of the Boost converter [A]
ΔV	input voltage ripple of step-up converter [V]
ΔV_o	output voltage ripple of step-up converter [V]
ΔI_L	inductor current ripple [A]

Greek letters

α	duty cycle

Abbreviations

FLC	Fuzzy Logic Control
INC	Incremental Conductance
LCD	Liquid Crystal Display
MPP	Maximum Power Point
MPPT	MPP Tracking
P & O	Perturb and Observe
PV	Photovoltaic
STC	Standard Test Condition

available.

On the other hand, researchers have proposed several MPPT algorithms in the literature (Verma et al., 2016). The criteria for selecting such MPPT algorithm are response time, steady-state oscillations, implementation complexity, and required sensors. The most popular MPPT algorithms are fuzzy logic control (FLC), artificial Neural Network (ANN), Perturb and observe (P&O) and INC. FLC and ANN techniques lead to a consistent MPPT due to their ability to manage the nonlinearity aspect of PV panels (Gounden et al., 2009; Lin et al., 2011b). For instance (Youssef et al., 2018), designed and implemented a FLC-MPPT on FPGA board. This controller can reach 98% efficiency (Messalti et al., 2017). designed and implemented a variable step size ANN-MPPT on DSP board. This controller can achieve an acceptable tracking accuracy and response time. However, the implementation of PV system based on artificial intelligence methods such as FLC and ANN is not easy due to their complexity. They require large memory for rules implementation and training, high-speed computing and high-level languages. This necessitates the use of expensive embedded boards as FPGA or DSP making the cost of PV system significantly high (Rezk and Eltamaly, 2015). Alternatively, the most commercialized MPPT algorithms are INC and P&O (Husain et al., 2017). P&O method is extensively employed in PV standalone systems due to its simplicity (Elgendy et al., 2012; Kamran et al., 2018; Killi and Samanta, 2015). In this kind of PV systems, it is preferred to implement MPPT algorithms using a low-cost microcontroller to reduce system expenses (Khaled et al., 2016). On the other side, INC is more complicated in operation compared with P&O since it contains several division computations that imply timely calculation process and the use of a stronger microcontroller (Motahhir et al., 2018a, 2017). Technically, P&O can make an inaccurate response which leads the system to oscillate around the MPP causing increased power losses (Abdelsalam et al., 2011; Femia et al., 2007, 2005; Piegari and Rizzo, 2010). For instance (Khaled et al., 2016), implemented a modified P&O in the cost-effective Freescale FRDM-KL25Z development board. The maximum reachable efficiency was 96%, a value that is unsatisfactory for effective utilization of PV systems. On the opposed side, INC is able to track rapidly the MPP with low steady-state oscillations during rapid changes of solar irradiations (Ishaque et al., 2014; Mishra and Sekhar, 2014; Radjai et al., 2014; Soon and Mekhilef, 2015, 2014).

This work aims to present a modified MPPT method with a simple structure and good performance. This method is a modification of the INC algorithm that eliminates all division computations rendering the algorithm simpler. This modification will ensure reduced real-time processing which makes the utilization of low-cost microcontrollers possible. Overall system simulation along with experimental validation are carried out to evaluate the technical feasibility and prove its superiority against the conventional technique. This system could be applicable for small or portable PV systems for which cost reductions can be critical for a wide use especially in low-income countries.

The rest of this paper is organized as follows: section 2 presents the modeling of the PV panel using Proteus. The modified INC algorithm is described in section 3. The implementation and the results of the proposed system are presented and discussed in Section 4. Finally, Section 5 outlines the main findings of this investigation.

2. Model of the photovoltaic panel using SPICE in Proteus

The PV panel can transform light from the sun into electrical energy by the photovoltaic effect. Fig. 1(a) shows the single-diode model of the PV panel. Other models have been proposed in the literature which are more refined and present high accuracy and serve several purposes. For instance, the two diode model is presented by (Gow and Manning, 1999; Nishioka et al., 2007) to include the impact of the recombination of carriers. For simplicity, the one diode model is used in this work. This model provides a good compromise between accuracy and simplicity [58], and has been used by several authors in previous works, sometimes with simplifications but always with the basic structure composed of a current source and a parallel diode (Ahmed and Salam, 2016; Faramarz et al., 2017; Kadri et al., 2012; Ram et al., 2018; Zakzouk et al., 2013; Zhou et al., 2014). The one-diode model is more suitable for power electronics designers who are looking for an easy and effective model for the simulation of PV panels with power converters.

As shown in Fig. 1(a), the single-diode model of the PV panel includes a source photon current Iph connected with a diode that emulates the P-N junction, as well as a shunt resistor Rsh and a series resistor Rs. Therefore, the PV current can be expressed by equation (1) (Chaibi et al., 2018):

$$I = I_{ph} - I_s\left\{\exp\left(\frac{V + IR_s}{aKTN_n}\right) - 1\right\} - \frac{V + R_sI}{R_{sh}} \quad (1)$$

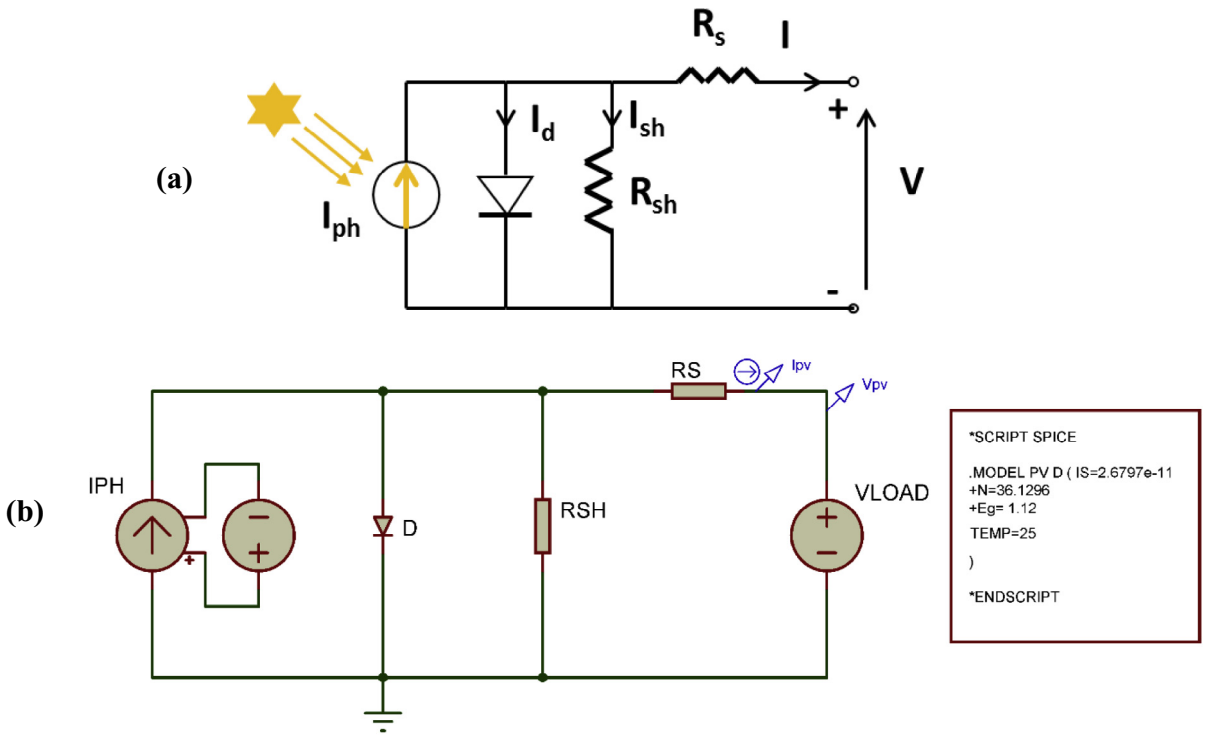

Fig. 1. (**a**): PV panel equivalent circuit, (**b**): Proteus model of the PV panel.

The TDC-M20-36 panel is employed in this study and Table 1 shows its specification. It should be mentioned that the missing parameters of the datasheet are extracted using the "PV array" tool provided by Mathworks as presented in (Motahhir et al., 2018b):

For modeling the photovoltaic panel in Proteus, its electrical model is designed as follows: a voltage controlled current source is connected in parallel with a diode (its SPICE code is modified according to the specification of the PV panel), then two resistors are bound in series and in parallel to model the shunt and the series resistors. Fig. 1(b) shows the Proteus model with its SPICE code. In addition, Fig. 2 presents the followed steps.

The test bench presented in Fig. 3(a) is built to validate the Proteus model. It consists of a PV panel, a variable load, a Pyranometer to measure the solar irradiation, a Multimeter to measure temperature, voltage and current sensors to measure voltage and current of the panel, and a computer to instrument the measured data by a virtual instrument made in LabVIEW tool (Hammoumi et al., 2018).

Fig. 3(b) presents the I-V and P-V curves for the proposed model in Proteus and experimental data at $T = 59\,^{\circ}C$ and $G = 920\,W/m^2$. As shown, the simulated data conform to the experimental data both in the current and power curves.

Once the PV panel is modeled in Proteus and validated, it can be employed to develop a PV system by implementing the MPPT controller using the hardware components provided by Proteus in its library, such as microcontrollers, DSP, FPGA, embedded boards like Arduino, sensors and actuators (Motahhir et al., 2017a). Therefore, it should be mentioned that the same MPPT C code developed through Proteus would be used for the physical prototype; this is the advantage of using Proteus, as opposed to Matlab/Simulink or PSIM, because the code of the algorithm would need to be rewritten for the physical prototype if we used Matlab/Simulink or PSIM. Hence, if such an algorithm is implemented in Proteus and the expected results are obtained, the physical prototype will likely obtain the same results due to the use of the same components during the simulation and physical implementation. On the other hand, since the objective of this study is to propose a low-cost PV system, Arduino Uno is used to implement and test the proposed MPPT algorithm due to its open-hardware nature and low cost.

Table 1
The TDC-M20-36 PV panel specifications at STC.

Characteristics	Values
MPP	20 W
V_{mp} (Voltage at MPP)	18.76 V
I_{mp} (Current at MPP)	1.07 A
I_{sc} (Short-circuit current)	1.17 A
V_{oc} (Open-circuit voltage)	22.7 V
K_v (Temperature Coefficient of V_{oc})	−0.35%/°C
Ki (Temperature Coefficient of I_{sc})	0.043%/°C
The number of cells, N_s	36
Light-generated current, I_{ph}	1.173 A
Diode saturation current, I_s	2.6797e-11 A
Ideality factor	1.0036
Shunt Resistance, R_{sh}	405.96 Ω
Series Resistance, R_s	1.0547 Ω

3. Modified INC algorithm

The conventional INC method is based on the incremental conductance (ΔI/ΔV) of the PV characteristics to identify the sign of P-V curve slope (ΔP/ΔV) and its structure can be presented as follows (Lin et al., 2011a):

$$\frac{\Delta P}{\Delta V} = 0 \text{ at MPP} \tag{2}$$

$$\frac{\Delta P}{\Delta V} > 0 \text{ left to MPP} \tag{3}$$

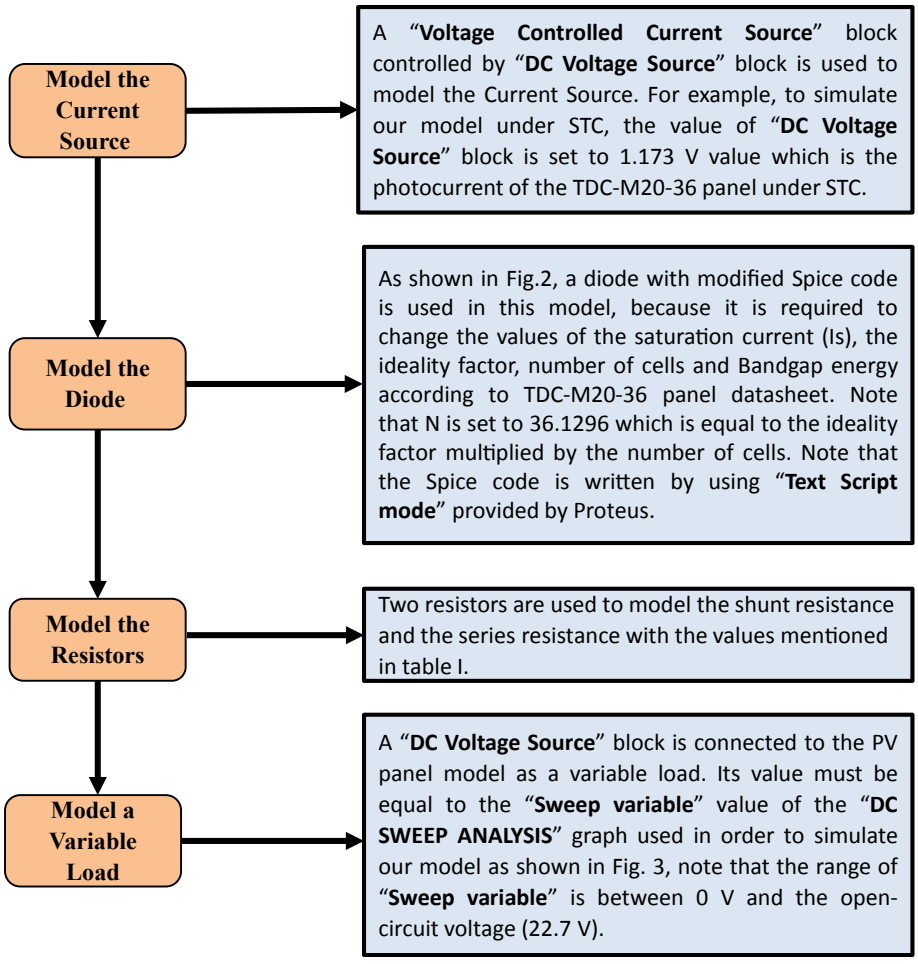

Fig. 2. Steps for modeling PV Panel in Proteus.

$$\frac{\Delta P}{\Delta V} < 0 \text{ right to MPP} \tag{4}$$

Since,

$$\frac{\Delta P}{\Delta V} = \frac{\Delta(IV)}{\Delta V} = V\frac{\Delta I}{\Delta V} + I \tag{5}$$

Therefore,

$$\frac{\Delta P}{\Delta V} = -\frac{I}{V} \text{ at MPP} \tag{6}$$

$$\frac{\Delta P}{\Delta V} > -\frac{I}{V} \text{ left to MPP} \tag{7}$$

$$\frac{\Delta P}{\Delta V} < -\frac{I}{V} \text{ right to MPP} \tag{8}$$

Based on equations (6)–(8), the conventional INC method is presented in Fig. 4 (Lin et al., 2011a).

As presented in Fig. 4, the conventional INC method contains several division computations which require a stronger microcontroller including large memory, high clock frequency, and floating-point computation, and this reduces the opportunity to use a low-cost development board (Motahhir et al., 2017b).

In this work, a modified INC algorithm is introduced. The latter avoids the high number of the mathematical divisions used in the conventional INC rendering the algorithm simpler. This modification will ensure reduced real-time processing which makes the utilization of low-cost microcontrollers possible (Zakzouk et al., 2013). Therefore, equations (6)–(8) are modified to be as follows:

$$\frac{[(V \times \Delta I) + (I \times \Delta V)]}{(\Delta V \times V)} = 0 \text{ at MPP} \tag{9}$$

$$\frac{[(V \times \Delta I) + (I \times \Delta V)]}{(\Delta V \times V)} > 0 \text{ left to MPP} \tag{10}$$

$$\frac{[(V \times \Delta I) + (I \times \Delta V)]}{(\Delta V \times V)} < 0 \text{ right to MPP} \tag{11}$$

The denominator of equations (9)–(11) is equal to V × ΔV. Since equation (9) since equation (9) is equal to zero, this denominator can be eliminated. As a result, the division is avoided for this equation as shown in (12). While only V can be removed from equations (10) and (11) because V is always greater than zero then it has no influence. Hence, the equations (13) and (14) are found:

$$(V \times \Delta I) + (I \times \Delta V) = 0 \text{ at MPP} \tag{12}$$

$$\frac{[(V \times \Delta I) + (I \times \Delta V)]}{\Delta V} > 0 \text{ left to MPP} \tag{13}$$

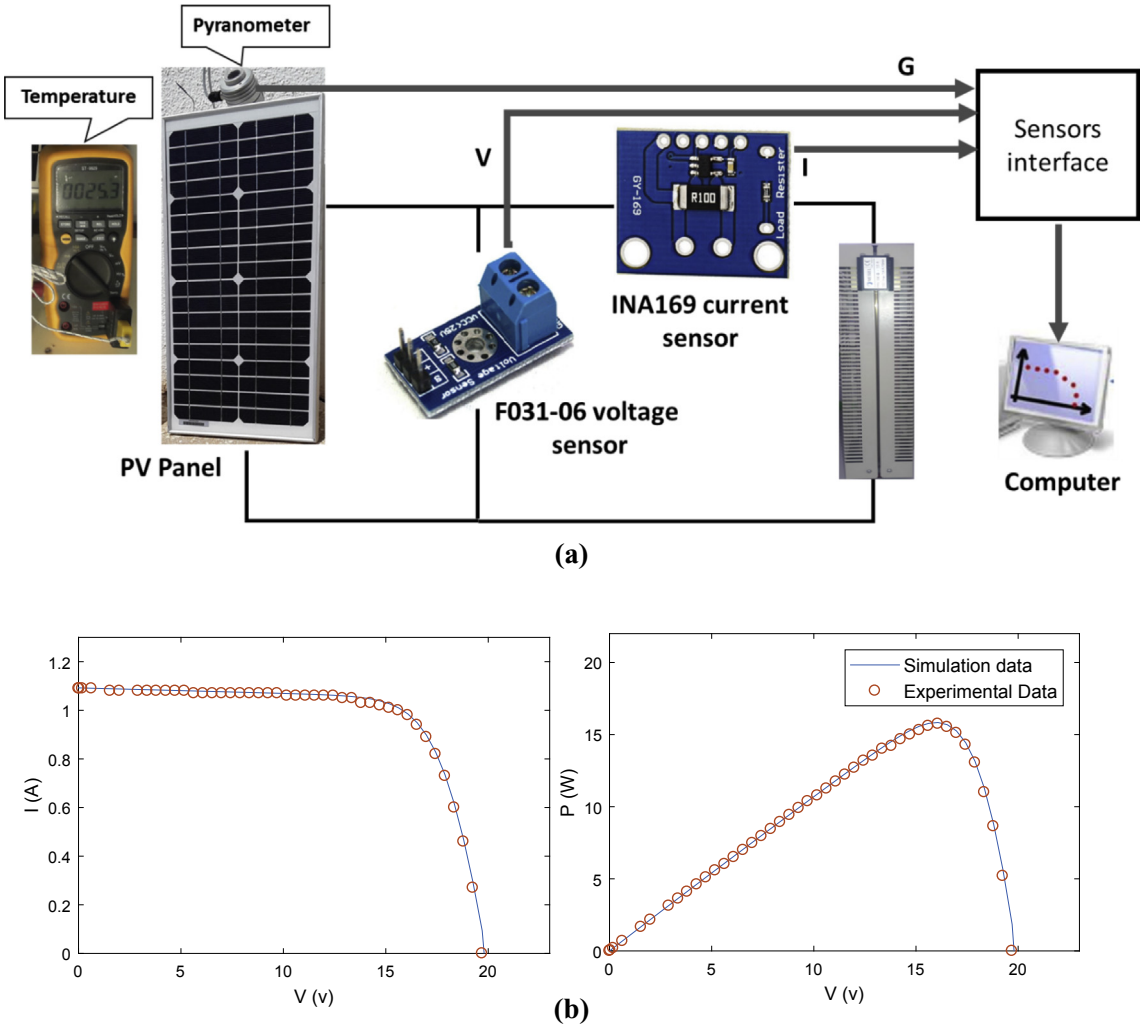

Fig. 3. (a): Measurement setup, (b): I-V and P-V characteristics for simulation and experimental data.

$$\frac{[(V \times \Delta I) + (I \times \Delta V)]}{\Delta V} < 0 \text{ right to MPP} \quad (14)$$

Moreover, to avoid the division calculations in equation (13) and (14), the logic "And" is used as follows in equations (16)–(19):

$$(V \times \Delta I) + (I \times \Delta V) = 0 \text{ at MPP} \quad (15)$$

$$(V \times \Delta I) + (I \times \Delta V) > 0 \text{ at MPP And left } \Delta V > 0 \text{ to MPP} \quad (16)$$

$$(V \times \Delta I) + (I \times \Delta V) < 0 \text{ at MPP } \Delta V < 0 \text{ And left to MPP} \quad (17)$$

$$(V \times \Delta I) + (I \times \Delta V) > 0 \text{ at MPP } \Delta V < 0 \text{ And right to MPP} \quad (18)$$

$$(V \times \Delta I) + (I \times \Delta V) < 0 \text{ at MPP And } \Delta V > 0 \text{ right to MPP} \quad (19)$$

The structure of the modified method is presented in Fig. 5, as shown the elimination of all division calculations is made using logic and arithmetic operations. As a result, the complication of the method operation is reduced and consequently, minimize the real-time processing which makes the utilization of low-cost micro-controllers possible.

Moreover, as shown in equation (15), the equality comparison is used to detect the MPP and then no more perturbation is induced in the duty cycle. However, the equality comparison between two reals cannot be precisely found by a controller because not all real numbers can be represented exactly by a controller (Goldberg, 1991). Therefore, as shown in the flowchart of the modified algorithm, a rounding error (0.06) is used with equation (15) to find the MPP, then stabilize the system at this point.

4. Implementation

4.1. Materials

Several components are used to implement the MPPT algorithm, such as voltage and current sensors, an embedded board, a converter, and a driver. Note that Proteus provides all these hardware components.

Embedded Board: Since the objective of this work is to design a low-cost PV system, Arduino UNO board, which is based on the low-cost ATMega328 microcontroller is employed in this work (Motahhir et al., 2017a).

Voltage sensor: is required to reduce the higher PV voltage to the Arduino analog input voltage, which is limited to 5 V. The sensor used in this work is "B25 Voltage Sensor Module" ("Voltage Sensor Module-Arduino Compatible," n.d.).

Current sensor: is required to sense the PV current. The sensor

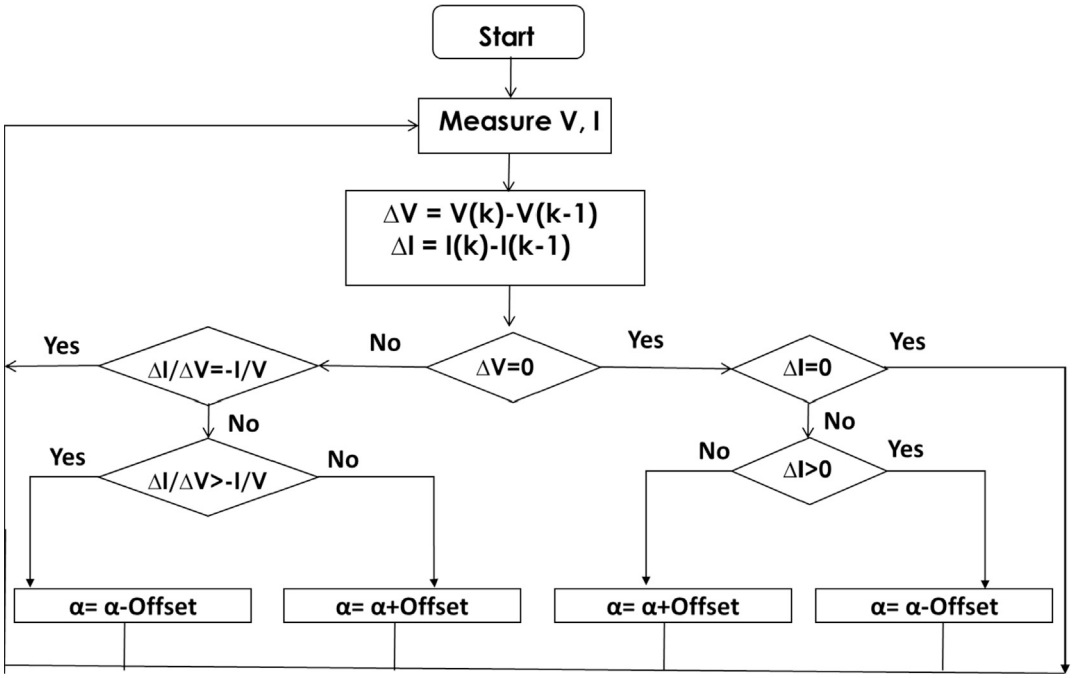

Fig. 4. Flowchart of INC method.

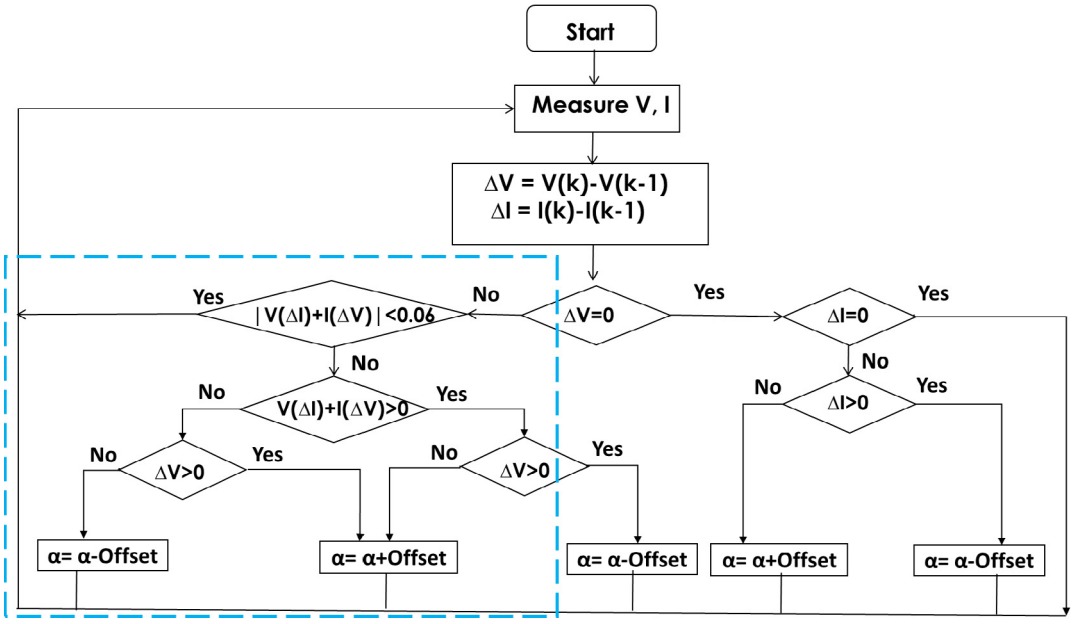

Fig. 5. Flowchart of the modified INC algorithm.

used in this work is "INA169 Analog DC Current Sensor" and it should be mentioned that its output voltage value equals to the value of the current that through it ("INA1x9 Datasheet," 2017).

Converter: as presented in Fig. 6, to remove the mismatch between the panel and the load and operate at MPP, the Boost converter is used in this work (Belkaid et al., 2016; Gayen and Jana, 2017; Montoya et al., 2016).

The Boost converter operates by the following equations (Motahhir et al., 2018b):

$$V_o = \frac{V}{(1-\alpha)} \tag{20}$$

$$I_o = I \times (1-\alpha) \tag{21}$$

The input capacitor value can be calculated as follows (Motahhir et al., 2018b):

$$C_{in} \geq \frac{\alpha}{8 \times F^2 \times L \times 0.01} \tag{22}$$

The output capacitor value may be computed as below (Motahhir et al., 2018b):

$$C_o \geq \frac{\alpha}{0.02 \times F \times R} \tag{23}$$

The inductance value must be designed as below, where r is the

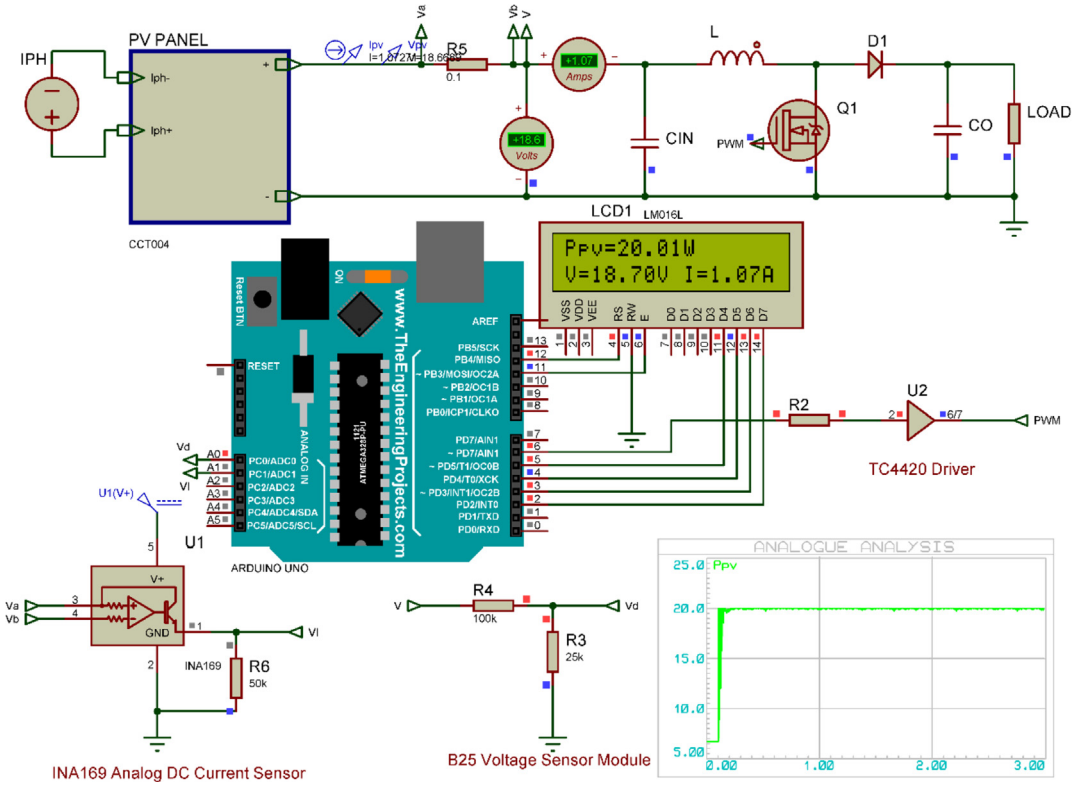

Fig. 6. Low-cost PV system designed in Proteus.

inductor current ripple ratio, which is optimal in the range of [0.3, 0.5] (Ayop and Tan, 2018; Motahhir et al., 2018b):

$$L \geq \frac{V \times \alpha}{r \times I \times F} \tag{24}$$

The parameters of the Boost converter are selected as follows, L = 20 mH, C_{in} = 220 μF, C_o = 470 μF, F = 1 kHz, and R of the load is 70 Ω. It should be mentioned that the switch used in the designed Boost is IRFP250N transistor because it has a low value of $R_dS(on)$ which is equal to 0.075 Ω. Therefore, by using this switch the loss of power is reduced. Furthermore, the Diode used is Schottky because it can increase the efficiency of the Boost converter due to its low forward voltage and its fast recovery time.

Driver: is used for controlling the MOSFET transistor by the microcontroller. The driver used in this work is TC4420; the latter is manufactured in CMOS for low consumption and more efficient working versus bipolar driver ("TC4420/TC4429 Datasheet," n.d.).

As depicted in Fig. 6, for clarity reasons the Proteus PV panel model is put in a "Subcircuit", then it is bound to the load through the Boost converter. The embedded board (Arduino) measures the PV voltage and current using voltage and current sensors. Next, the MPPT algorithm implemented in the embedded board uses these data to control the Boost converter through the driver by using the computed duty cycle to reach the MPP. Moreover, the PV power, voltage and current are displayed on the LCD screen.

4.2. Results and discussion

4.2.1. Simulation result

The simulation was made to compare the dynamic and the steady-state performance of the INC and the modified INC methods. In addition, the execution time of both methods is compared to show the benefit of eliminating all division calculations in the modified method. Therefore, Fig. 7(a) presents the execution time of the conventional INC program which is 480 μs and Fig. 7(b) presents the execution time of the modified method which is 300 μs. Hence, the elimination of all division computation in the modified method renders the process simpler which reduces the real-time processing.

The insolation is suddenly changed from 1000 W/m^2 to 500 W/m^2 at t = 1.5 s. Fig. 8(a) presents simulation result of the conventional algorithm and Fig. 8(b) presents simulation result of the modified algorithm. As presented in these figures, the steady-state oscillations are decreased by using the modified algorithm. Moreover, when the irradiation is modified, the response time is 0.37 s for the conventional algorithm and 0.1 s for the modified algorithm. Hence, the elimination of all division computation in the modified method enhances the performance with low steady-state oscillations and fast-tracking speed.

4.2.2. Experimental result

The elimination of all division computation in the modified algorithm results in simplifying its construction and makes the utilization of low-cost microcontrollers possible with enhancing its performance. To validate that, a test bench using real hardware components is built.

Both methods are implemented in the ATMega328 microcontroller. Fig. 9 shows the experimental setup, and as presented, a computer is used to instrument the PV power by using a virtual instrument made by "Instrument Control Toolbox" of Matlab Simulink. Moreover, a brutal decrease in solar irradiance should be made to compare the dynamic response of both algorithms. However, PV panels are unable to generate this profile due to randomly environmental meteorological data. Therefore, as presented in Fig. 9, it is necessary to replace the PV panel by PV Emulator. This emulator is based only on a simple DC power supply and two

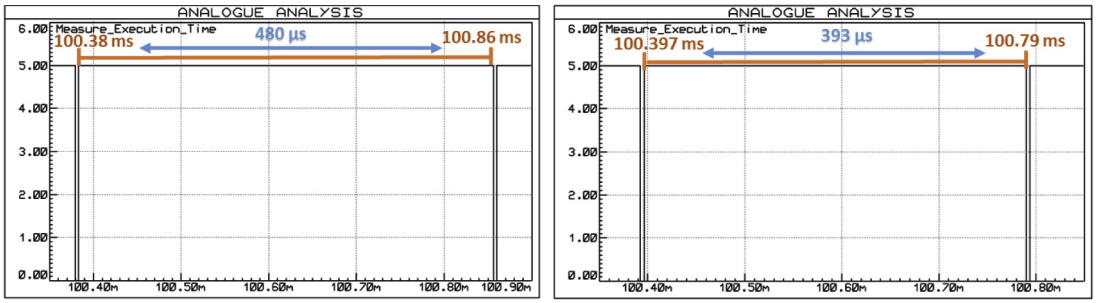

(a) (b)

Fig. 7. **(a)**: Execution time of the conventional method program, **(b)**: Execution time of the modified method program.

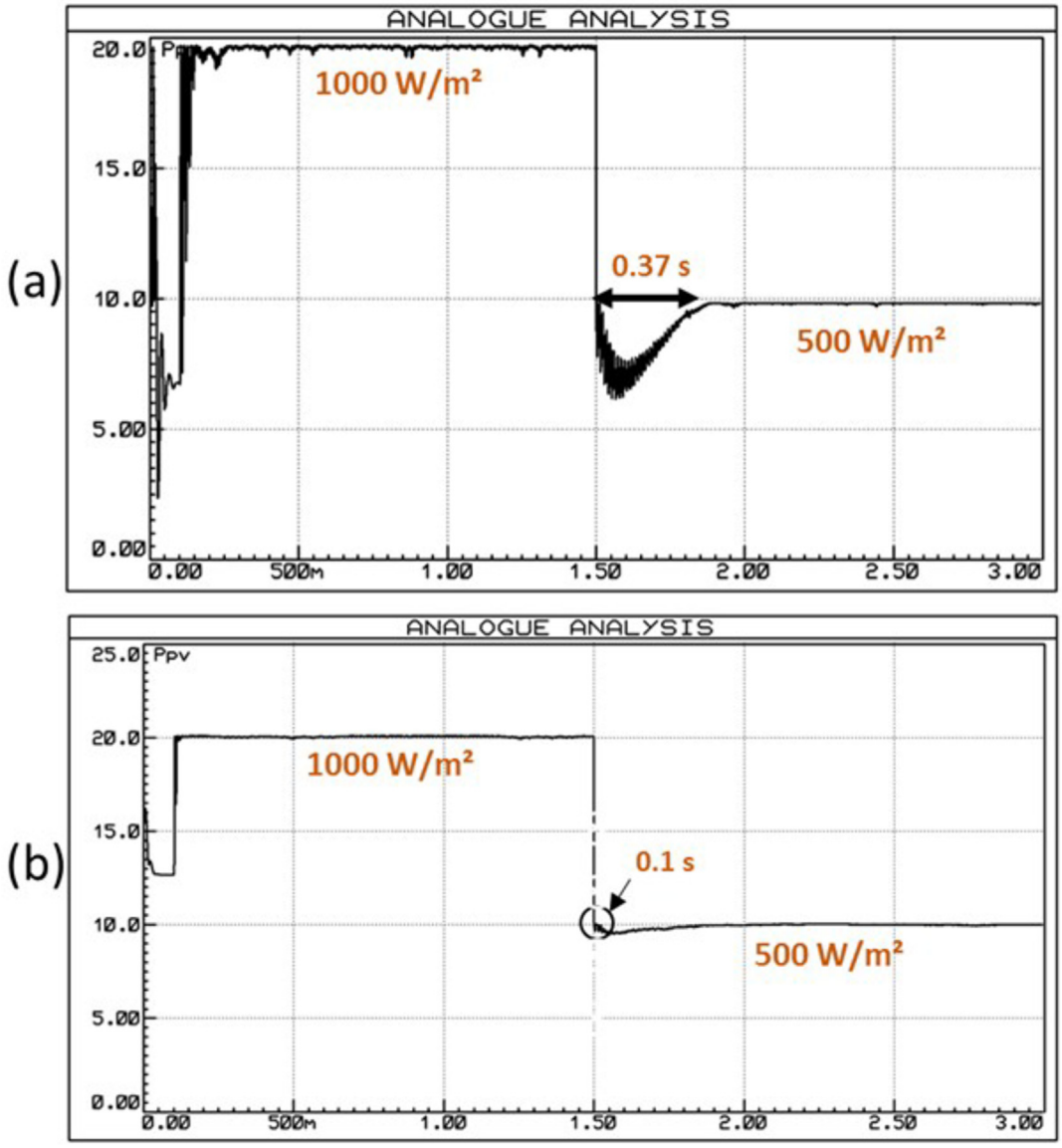

Fig. 8. **(a)**: Simulation result of the conventional INC algorithm, **(b)**: Simulation result of the modified INC algorithm.

resistors as reported by (Ram et al., 2018) and these components are often available. Therefore, this emulator does not require any financial burden.

Fig. 10(a) and (b) present the experimental results of both methods under fast varying of insolation (from 1000 W/m^2 to 500 W/m^2). A zoom in the results is made. As shown in Fig. 10(a), the conventional method generates more oscillations around the peak of power compared to the modified method as presented in

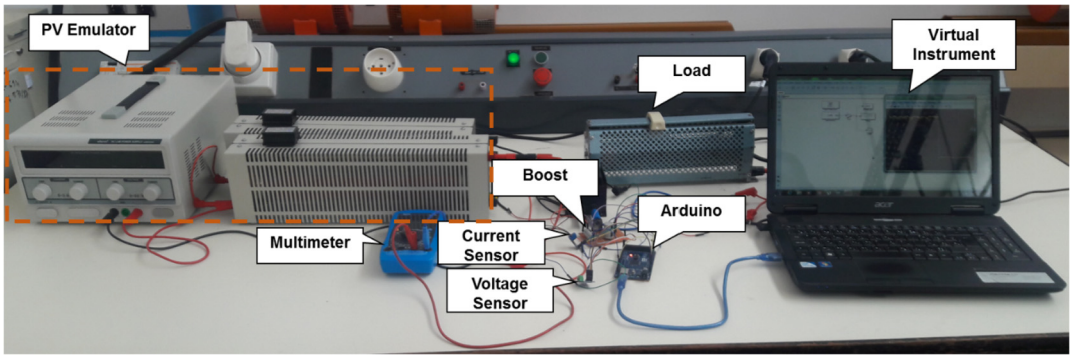

Fig. 9. Experimental setup.

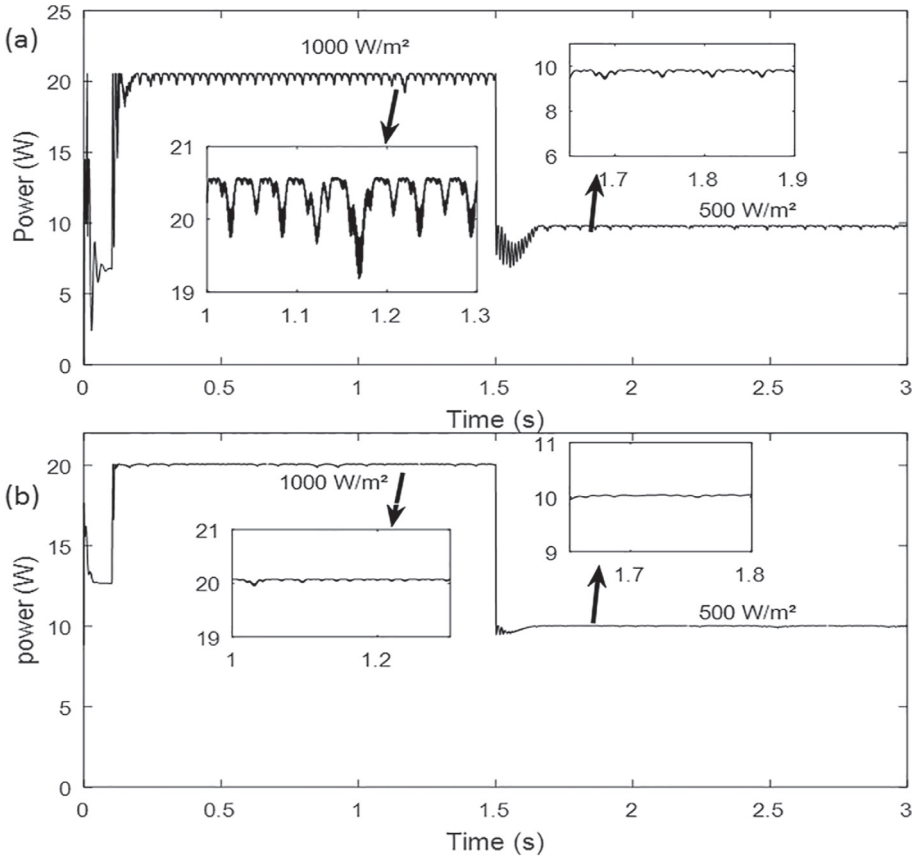

Fig. 10. **(a)**: Experimental result of the conventional INC algorithm, **(b)**: Experimental result of the modified INC algorithm.

Fig. 10(b). On the other hand, the modified method presents a faster tracking speed with response time equals to 0.1 s which is very lower than the response time obtained by the conventional method (0.36 s).

In brief, experimental results validate that the modified algorithm decreases the execution time of the controller, which results in the best compromise between steady-state performance and faster response. As shown in Table 2, the proposed work is compared with some experimental works published recently. It should be mentioned that they do not refer to the same conditions since it is very difficult to find several works done under the same conditions. so if we compare the proposed work with low-cost microcontrollers' implementation (Mishra and Sekhar, 2014), our solution presents a faster response to a sudden change. Whereas, prototypes with faster response use an expensive controller (FPGA or DSP) (Chavoshian et al., 2014; Rahim et al., 2014). Thus, an expensive controller (dSPACE) is used by (Boukenoui et al., 2017), nevertheless, this work presents a slower response time compared to our proposal. In addition, our system presents a neglected steady-state oscillation. Moreover, it presents one of the highest efficiencies of more than 98%.

Consequently, the modified INC algorithm implemented by the low-cost ATMega328 microcontroller results in the best compromise between steady-state and dynamic performances. Hence, the proposed system could be applicable for small or portable PV systems for which cost reductions can be critical for a wide use especially in low-income countries.

Table 2
Comparison between our proposal and some experimental works published recently.

Publication year, Paper	PV Power at STC	MPPT algorithm	Embedded Controller	Power ripples	Efficiency	Response time	Cost of controller	Conditions of test
(Chavoshian et al., 2014)	80 W	Modified INC	FPGA (Xilinx XC3S400)	2.7 W	98.8%	2.5 ms	38.5 $	500 and 900 W/m^2, 38 °C
(Rahim et al., 2014)	210 W	Adaptive P&O-fuzzy MPPT	DSP TMS320F28335	1 W	95.2%	20 ms	21.17 $	200 and 1000 W/m^2
(Mishra and Sekhar, 2014)	40 W	TS fuzzy-based INC	dsPIC33fJ128MC802	1 W	97.5%	2 s	4.46 $	500 and 1000 W/m^2
(Soon and Mekhilef, 2015)	87 W	Modified INC	Microcontroller PIC18f410	1.3 W	99%	0.275 s	4.26 $	400 and 1000 W/m^2, 25 °C
(Boukenoui et al., 2017)	10 W	FLC MPPT	dSPACE-1103	0.9 W	97.295%	0.264 s	38 $	(858 W/m^2 26 °C) and (493 W/m^2 19 °C)
(Boukenoui et al., 2017)	10 W	Improved INC	dSPACE-1103	1 W	91.93%	0.254 s	38 $	858 W/m^2 26 °C) and (493 W/m^2 19 °C)
Proposed	20 W	Modified INC	Atmega 328	0.5 W	98.5%	0.1 s	2 $	500 and 1000 W/m^2, 25 °C

5. Conclusions

For the first time, a validated Proteus PV panel model is developed and presented in this work. subsequently, this PV model and the hardware components available in Proteus can be used as a low-cost PV simulator to implement and verify the performance of MPPT algorithms when the physical prototype is not available. This simulator makes future modifications to the system much easier to achieve.

Moreover, a modified INC algorithm is presented through the elimination of all division computations occurring in the conventional INC method. A simpler structure is obtained making the implementation of low-cost microcontrollers easy while minimizing the system cost. Based on simulation and experimental results, it can be concluded that the modified method is able to track correctly the MPP with faster response and low steady-state oscillations under sudden change compared to conventional INC algorithms. Wherefore, the proposed system can constitute a suitable low-cost solution for PV power generation systems.

It should be highlighted that the result obtained by Proteus simulation is nearly the same obtained by the experimental work. Thus, we can rely on this Proteus test bench to verify the performance of such MPPT algorithm.

Acknowledgments

The authors would like to thank the anonymous reviewers for their helpful and constructive comments that greatly contributed to improving the final version of the paper. They would also like to thank the Editors for their generous comments and support during the review process.

References

Abdelsalam, A.K., Massoud, A.M., Ahmed, S., Enjeti, P.N., 2011. High-performance adaptive Perturb and observe MPPT technique for photovoltaic-based microgrids. IEEE Trans. Power Electron. https://doi.org/10.1109/TPEL.2011.2106221.

Ahmed, J., Salam, Z., 2016. A modified P and O Maximum power point tracking method with reduced steady-state oscillation and improved tracking efficiency. IEEE Trans. Sustain. Energy. https://doi.org/10.1109/TSTE.2016.2568043.

Ayop, R., Tan, C.W., 2018. Design of boost converter based on maximum power point resistance for photovoltaic applications. Sol. Energy 160, 322–335. https://doi.org/10.1016/J.SOLENER.2017.12.016.

Bayrak, F., Ertürk, G., Oztop, H.F., 2017. Effects of partial shading on energy and exergy efficiencies for photovoltaic panels. J. Clean. Prod. 164, 58–69. https://doi.org/10.1016/J.JCLEPRO.2017.06.108.

Belkaid, A., Colak, I., Isik, O., 2016. Photovoltaic maximum power point tracking under fast varying of solar radiation. Appl. Energy 179, 523–530. https://doi.org/10.1016/J.APENERGY.2016.07.034.

Boukenoui, R., Ghanes, M., Barbot, J.-P., Bradai, R., Mellit, A., Salhi, H., 2017. Experimental assessment of maximum power point tracking methods for photovoltaic systems. Energy 132, 324–340. https://doi.org/10.1016/J.ENERGY.2017.05.087.

Chaibi, Y., Salhi, M., El-jouni, A., Essadki, A., 2018. A new method to extract the equivalent circuit parameters of a photovoltaic panel. Sol. Energy 163, 376–386. https://doi.org/10.1016/J.SOLENER.2018.02.017.

Chavoshian, M.R., Rouholamini, A., Naji, H.R., Fadaeinedjad, R., Faraji, R., 2014. FPGA-based real time incremental conductance maximum power point tracking controller for photovoltaic systems. IET Power Electron. https://doi.org/10.1049/iet-pel.2013.0603.

Chen, Y.-T., Jhang, Y.-C., Liang, R.-H., 2016. A fuzzy-logic based auto-scaling variable step-size MPPT method for PV systems. Sol. Energy 126, 53–63. https://doi.org/10.1016/J.SOLENER.2016.01.007.

Elgendy, M.A., Zahawi, B., Atkinson, D.J., 2012. Assessment of perturb and observe MPPT algorithm implementation techniques for PV pumping applications. IEEE Trans. Sustain. Energy. https://doi.org/10.1109/TSTE.2011.2168245.

Faramarz, Amiri, M., Zarchi, H.A., 2017. Two-switch flyback inverter employing a current sensorless MPPT and scalar control for low cost solar powered pumps. IET Renew. Power Gener 11, 669–677.

Femia, N., Petrone, G., Spagnuolo, G., Vitelli, M., 2005. Optimization of perturb and observe maximum power point tracking method. IEEE Trans. Power Electron. https://doi.org/10.1109/TPEL.2005.850975.

Femia, N., Granozio, D., Petrone, G., Spagnuolo, G., Vitelli, M., 2007. Predictive & adaptive MPPT perturb and observe method. IEEE Trans. Aero. Electron. Syst. https://doi.org/10.1109/TAES.2007.4383584.

Gayen, P.K., Jana, A., 2017. An ANFIS based improved control action for single phase utility or micro-grid connected battery energy storage system. J. Clean. Prod. 164, 1034–1049. https://doi.org/10.1016/J.JCLEPRO.2017.07.007.

Goldberg, D., 1991. What every computer scientist should know about floating-point arithmetic. ACM Comput. Surv. https://doi.org/10.1145/103162.103163.

Gounden, N.A., Ann Peter, S., Nallandula, H., Krithiga, S., 2009. Fuzzy logic controller with MPPT using line-commutated inverter for three-phase grid-connected photovoltaic systems. Renew. Energy 34, 909–915. https://doi.org/10.1016/J.RENENE.2008.05.039.

Gow, J.A., Manning, C.D., 1999. Development of a photovoltaic array model for use in power-electronics simulation studies. IEE Proc. Elec. Power Appl. https://doi.org/10.1049/ip-epa:19990116.

Gupta, A., Chauhan, Y.K., Pachauri, R.K., 2016. A comparative investigation of maximum power point tracking methods for solar PV system. Solar Energy. Pergamon.

Hammoumi, A.E., Motahhir, S., Chalh, A., Ghzizal, A.E., Derouich, A., 2018. Real-time virtual instrumentation of Arduino and LabVIEW based PV panel characteristics. In: IOP Conference Series: Earth and Environmental Science. https://doi.org/10.1088/1755-1315/161/1/012019.

Husain, M.A., Tariq, A., Hameed, S., Arif, M.S. Bin, Jain, A., 2017. Comparative assessment of maximum power point tracking procedures for photovoltaic systems. Green Energy Environ 2, 5–17. https://doi.org/10.1016/J.GEE.2016.11.001.

INA1x9 Datasheet [WWW Document], 2017. URL www.ti.com (accessed 8.1.18).

Ishaque, K., Salam, Z., Lauss, G., 2014. The performance of perturb and observe and incremental conductance maximum power point tracking method under dynamic weather conditions. Appl. Energy 119, 228–236. https://doi.org/10.1016/J.APENERGY.2013.12.054.

Kadri, R., Gaubert, J.-P., Ivanovici, T., Champenois, G., Andrei, P., 2012. Modeling of the photovoltaic cell circuit parameters for optimum connection model and real-time emulator with partial shadow conditions. Energy 42, 57–67. https://doi.org/10.1016/J.ENERGY.2011.10.018.

Kamran, M., Mudassar, M., Fazal, M.R., Asghar, M.U., Bilal, M., Asghar, R., 2018. Implementation of improved Perturb & Observe MPPT technique with confined search space for standalone photovoltaic system. J. King Saud Univ. - Eng. Sci. https://doi.org/10.1016/J.JKSUES.2018.04.006.

Khaled, M., Ali, H., Abd-El Sattar, M., Elbaset, A.A., 2016. Implementation of a modified perturb and observe maximum power point tracking algorithm for photovoltaic system using an embedded microcontroller. IET Renew. Power

Gener. https://doi.org/10.1049/iet-rpg.2015.0309.
Killi, M., Samanta, S., 2015. Modified perturb and observe MPPT algorithm for drift avoidance in photovoltaic systems. IEEE Trans. Ind. Electron. https://doi.org/10.1109/TIE.2015.2407854.
Koofigar, H.R., 2016. Adaptive robust maximum power point tracking control for perturbed photovoltaic systems with output voltage estimation. ISA Trans. 60, 285–293. https://doi.org/10.1016/J.ISATRA.2015.11.003.
Li, Q., Zhao, S., Wang, M., Zou, Z., Wang, B., Chen, Q., 2017. An improved perturbation and observation maximum power point tracking algorithm based on a PV module four-parameter model for higher efficiency. Appl. Energy 195, 523–537. https://doi.org/10.1016/J.APENERGY.2017.03.062.
Lin, C.-H., Huang, C.-H., Du, Y.-C., Chen, J.-L., 2011a. Maximum photovoltaic power tracking for the PV array using the fractional-order incremental conductance method. Appl. Energy 88, 4840–4847. https://doi.org/10.1016/J.APENERGY.2011.06.024.
Lin, W.M., Hong, C.M., Chen, C.H., 2011b. Neural-network-based MPPT control of a stand-alone hybrid power generation system. IEEE Trans. Power Electron. https://doi.org/10.1109/TPEL.2011.2161775.
Marinić-Kragić, I., Nižetić, S., Grubišić-Čabo, F., Papadopoulos, A.M., 2018. Analysis of flow separation effect in the case of the free-standing photovoltaic panel exposed to various operating conditions. J. Clean. Prod. 174, 53–64. https://doi.org/10.1016/J.JCLEPRO.2017.10.310.
Messalti, S., Harrag, A., Loukriz, A., 2017. A new variable step size neural networks MPPT controller: review, simulation and hardware implementation. Renew. Sustain. Energy Rev. 68, 221–233. https://doi.org/10.1016/J.RSER.2016.09.131.
Mishra, S., Sekhar, P.C., 2014. Takagi–Sugeno fuzzy-based incremental conductance algorithm for maximum power point tracking of a photovoltaic generating system. IET Renew. Power Gener. https://doi.org/10.1049/iet-rpg.2013.0219.
Montoya, D.G., Ramos-Paja, C.A., Giral, R., 2016. Improved design of sliding-mode controllers based on the requirements of MPPT techniques. IEEE Trans. Power Electron. https://doi.org/10.1109/TPEL.2015.2397831.
Motahhir, S., Ghzizal, A. El, Sebti, S., Derouich, A., 2017a. MIL and SIL and PIL tests for MPPT algorithm. Cogent Eng 4. https://doi.org/10.1080/23311916.2017.1378475.
Motahhir, S., Chalh, A., El Ghzizal, A., Sebti, S., Derouich, A., 2017b. Modeling of photovoltaic panel by using proteus. J. Eng. Sci. Technol. Rev. 10, 8–13. https://doi.org/10.25103/jestr.102.02.
Motahhir, S., El Hammoumi, A., El Ghzizal, A., 2018a. Photovoltaic system with quantitative comparative between an improved MPPT and existing INC and P&O methods under fast varying of solar irradiation. Energy Rep. 4, 341–350. https://doi.org/10.1016/J.EGYR.2018.04.003.
Motahhir, S., Ghzizal, A. El, Sebti, S., Derouich, A., 2018b. Modeling of photovoltaic system with modified incremental conductance algorithm for fast changes of irradiance. Int. J. Photoenergy. https://doi.org/10.1155/2018/3286479.
Nishioka, K., Sakitani, N., Uraoka, Y., Fuyuki, T., 2007. Analysis of multicrystalline silicon solar cells by modified 3-diode equivalent circuit model taking leakage current through periphery into consideration. Sol. Energy Mater. Sol. Cells 91, 1222–1227. https://doi.org/10.1016/J.SOLMAT.2007.04.009.
Nižetić, S., Arıcı, M., Bilgin, F., Grubišić-Čabo, F., 2018. Investigation of pork fat as potential novel phase change material for passive cooling applications in photovoltaics. J. Clean. Prod. 170, 1006–1016. https://doi.org/10.1016/J.JCLEPRO.2017.09.164.
Piegari, L., Rizzo, R., 2010. Adaptive perturb and observe algorithm for photovoltaic maximum power point tracking. IET Renew. Power Gener. https://doi.org/10.1049/iet-rpg.2009.0006.
Radjai, T., Rahmani, L., Mekhilef, S., Gaubert, J.P., 2014. Implementation of a modified incremental conductance MPPT algorithm with direct control based on a fuzzy duty cycle change estimator using dSPACE. Sol. Energy 110, 325–337. https://doi.org/10.1016/J.SOLENER.2014.09.014.
Rahim, N.A., Che Soh, A., Radzi, M.A.M., Zainuri, M.A.A.M., 2014. Development of adaptive perturb and observe-fuzzy control maximum power point tracking for photovoltaic boost dc–dc converter. IET Renew. Power Gener. https://doi.org/10.1049/iet-rpg.2012.0362.
Rahrah, K., Rekioua, D., Rekioua, T., Bacha, S., 2015. Photovoltaic pumping system in Bejaia climate with battery storage. Int. J. Hydrogen Energy 40, 13665–13675. https://doi.org/10.1016/J.IJHYDENE.2015.04.048.
Ram, J.P., Manghani, H., Pillai, D.S., Babu, T.S., Miyatake, M., Rajasekar, N., 2018. Analysis on solar PV emulators: a review. Renew. Sustain. Energy Rev. 81, 149–160. https://doi.org/10.1016/J.RSER.2017.07.039.
Rezk, H., Eltamaly, A.M., 2015. A comprehensive comparison of different MPPT techniques for photovoltaic systems. Sol. Energy 112, 1–11. https://doi.org/10.1016/J.SOLENER.2014.11.010.
Soon, T.K., Mekhilef, S., 2014. Modified incremental conductance MPPT algorithm to mitigate inaccurate responses under fast-changing solar irradiation level. Sol. Energy 101, 333–342. https://doi.org/10.1016/J.SOLENER.2014.01.003.
Soon, T.K., Mekhilef, S., 2015. A fast-converging MPPT technique for photovoltaic system under fast-varying solar irradiation and load resistance. IEEE Trans. Ind. Informatics. https://doi.org/10.1109/TII.2014.2378231.
TC4420/TC4429 Datasheet [WWW Document], n.d. URL http://ww1.microchip.com/downloads/en/DeviceDoc/21419D.pdf (accessed 8.1.18).
Verma, D., Nema, S., Shandilya, A.M., Dash, S.K., 2016. Maximum power point tracking (MPPT) techniques: recapitulation in solar photovoltaic systems. Renew. Sustain. Energy Rev. 54, 1018–1034. https://doi.org/10.1016/J.RSER.2015.10.068.
Voltage Sensor Module-Arduino Compatible [WWW Document], n.d. URL https://www.emartee.com/product/42082/Voltage Sensor (accessed 8.1.18).
Youssef, A., Telbany, M. El, Zekry, A., 2018. Reconfigurable generic FPGA implementation of fuzzy logic controller for MPPT of PV systems. Renew. Sustain. Energy Rev. 82, 1313–1319. https://doi.org/10.1016/J.RSER.2017.09.093.
Zakzouk, N.E., Abdelsalam, A.K., Helal, A.A., Williams, B.W., 2013. Modified variable-step incremental conductance maximum power point tracking technique for photovoltaic systems. In: IECON Proceedings (Industrial Electronics Conference). https://doi.org/10.1109/IECON.2013.6699395.
Zhou, Z., Holland, P.M., Igic, P., 2014. MPPT algorithm test on a photovoltaic emulating system constructed by a DC power supply and an indoor solar panel. Energy Convers. Manag. 85, 460–469. https://doi.org/10.1016/J.ENCONMAN.2014.06.007.